LaCo$_{0.5}$Fe$_{0.5}$O3 Nanoparticles as a Highly Efficient Adsorbent for Rapid Removal of Trypan Blue Dye From Aqueous Media

Mojtaba Ershadi, Haman Tavakkoli[*], Arezoo Ghaemi, Afruz Azarkish

Department of Chemistry, Ahvaz Branch, Islamic Azad University, Ahvaz, Iran

(Received 09 Mar. 2017; Final version received 10 Jun. 2017)

Abstract

Nanoparticles of perovskite-type LaCo$_{0.5}$Fe$_{0.5}$O$_3$ (LCFO) were fabricated by sol–gel method. Thermal decomposition process of the complex precursor was examined by means of differential thermal analysis–thermal gravimetric analysis (DTA/TGA). X-ray diffraction (XRD) results showed that single perovskite phase has been completely formed after calcination at 750 $^\circ$C. In addition, the surface morphology and composition of these nanopowders were also investigated using SEM and EDX. These nanoparticles showed the excellent adsorption efficiency towards Trypan Blue (TB) as a reactive dye in aqueous solution. The adsorption studies were carried out at different pH values, dye concentrations, various adsorbent dosages and contact time in a batch experiments. LCFO exhibited good dye removal efficiency at acidic pH specially pH 2. Experimental results indicated that the adsorption kinetic data follow a pseudo-second-order rate for tested dye. The isotherm evaluations revealed that the Freundlich model better fits to the experimental equilibrium data than Langmuir the model.

Keywords: Perovskite, Nanoparticles, Sol-gel, Dye Removal, Trypan Blue.

*****Corresponding author**: Haman Tavakkoli, Department of Chemistry, Ahvaz Branch, Islamic Azad University, Ahvaz, Iran. E-mail address: htavakkoli59@gmail.com, Tel: +98-611-4457612, Fax: +98-611-4435288.*

Introduction

Textile industry is one of those industries that consume large amounts of water in the manufacturing process [1] and, also, discharge great amounts of effluents with synthetic dyes to the environment causing public concern and legislation problems. Synthetic dyes that make up the majority (60–70%) of the dyes applied in textile processing industries [2] are considered tobe serious health risk factors. Apart from the aesthetic deterioration of water bodies, many colorants and their breakdown products are toxic to aquatic life [3] and can cause harmful effects to humans [4,5]dyes are organic compounds consisting of two main groups of compounds, chromophores (responsible for color of the dye) and auxochromes (responsible for intensity of the color) [6]. Many processes are employed to remove dye molecules from colored effluents; in general, treatment methods can be divided into three categories: (i) physical methods such as adsorption [7-9], and membrane filtration [10],(ii) chemical methods such as ionic exchange [11], chemical oxidation [12,13],electrochemical degradation [14], and ozonation [15],and (iii) biological degradation [16].The traditional physical, chemical and biologic means of wastewater treatment often have little degradation effect on this kind of pollutants. On the contrary, the technology of nanoparticulate photodegradation has been proved to be effective to them. Compared with the other conventional wastewater treatment means, this technology has such advantages as: (1) wide application, especially to the molecule structure-complexed contaminants which cannot be easily degraded by the traditional methods; (2) the nanoparticles itself have no toxicity to the health of our human livings and (3) it demonstrates a strong destructive power to the pollutants and can mineralize the pollutants into CO_2 and H_2O. Due to the excellent features of this technology, it appears promising and has drawn the attention of researchers of at home and abroad [17-19].

Perovskite oxides have caused great interests and have been widely studied for their various properties and application in the recent decades. They can be used as superconductors, and the critical temperature decreases linearly with increasing A-site disorder, as quantified by the variance in the distribution of A-site cation radii. The critical temperature is also very sensitive to lattice strains [20-23]. In the present study, $LaCo_{0.5}Fe_{0.5}O_3$ (LCFO) component with perovskite structure was prepared via the sol-gel method and characterized by different techniques such as XRD, FTIR, SEM and DTA/TGA. Moreover, its efficiency as an adsorbent for removal of diazo dye, Trypan Blue (TB), from an aqueous solution was evaluated. The effect of different variables

including concentration of dye, different pH values, adsorbent doses and reaction time, for removal of TB on LCFO nanopowders has been investigated and two kinetic models have also been analyzed. Furthermore, preparation of LCFO nanoparticlesvia sol–gel method and its characterization by different techniques such as DTA, TGA, XRD, SEM, EDX and FTIR have been reported.

Experimental

General remarks

La(NO$_3$)$_3$.6H$_2$O (99.99% purity), Co(NO$_3$)$_2$.6H$_2$O (99.99% purity), Fe(NO$_3$)$_3$.9H$_2$O (99.99% purity) were all obtained from Merck, Germany; Citric acid (CA) (99.5% purity), was purchased from Aldrich, USA. The commercial color index (CI) diazo dye (TB, molecular weight = 872.88 g/mol) was generously provided by Sigma company, USA which was used without further purification (Figure 1). All the reagents were of analytical grade and thus used as received. Deionized water was used throughout the experiments.
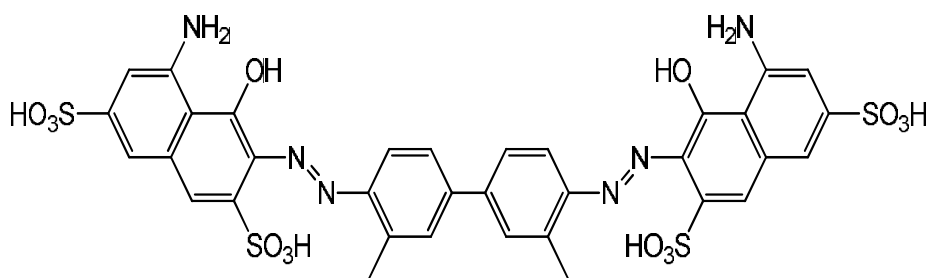

Figure 1. Molecular structure of Trypan Blue (TB) dye.

Preparation and characterization of LaCo$_{0.5}$Fe$_{0.5}$O$_3$

For the preparation of the nanoperovskite in this work, the aqueous solutions of metal nitrates with nominal atomic ratios La:Co:Fe=1:0.5:0.5 were dissolved in 20 ml of deionized water, Citric acid (CA) was proportionally added to the metal solution by stirring at room temperature. The solution was concentrated by evaporation at approximately 75°C to remove excess water. Then, the dry gel was obtained by letting the sol into an oven and heated slowly up to 110°C and kept for 18 h in baking oven. Then, it was ground in agate mortar and turned into powder and

calcinated at 750°C in air for 9 h. The annealing of the amorphous precursor allows removing most of the residual carbon and the orthorhombic perovskite phase was obtained.

The decomposition and reaction processes of the dried gel have been analyzed by (DTA) and (TGA) using a STA 503, Germany, in the range of room temperature to 1000 $^{\circ}$C, in air with a heating rate of 10 $^{\circ}$C/min. The complex polymeric gel and derived powders have been also analyzed by (FTIR) spectroscopy on Perkin Elmer BX II FTIR spectrometer. The crystallization and microstructure of the oxide powders have been characterized with an X-ray diffractometer employing a scanning rate of 0.02 S^{-1} in a 2θ range from 20 to 70°C, using a X́ pert, 200, Equinox 3000, France, equipped with CuK$_{\alpha}$ radiation. The morphology and chemical analysis of the particles was investigated using (SEM) and (EDX) technique. The SEM of the type KYKY EM3200 (V = 30 kV) EDX spectrometer of the type Inca 400 (Oxford Instruments). A UV–Vis spectrophotometer (Perkin Elmer lambda 35) was employed to monitor adsorption of dyes.

Dye removal experiments

A prepared solution of Trypan Blue (TB) was distributed into different flasks (1 L capacity) and pH was adjusted with the help of the pH meter (HORIBA F 11 E, Japan made). The initial pH value of the dye solution was adjusted to the desired levels, using either HCl (0.5 M) or NaOH (0.5 M). A known mass of nano-LCFO powder (Adsorbent dosage) was then added to 10 mL of the TB aqueous solution, and the obtained suspension was immediately stirred for a predefined time. All experiments were done at the room temperature. The investigated ranges of the experimental variables were as follows: dye concentration (50-250 mg/L), pH of solution (2-12), Adsorbent dosage (0.005, 0.01 and 0.02 g) and mixing time (2- 20 min). After a preselected time of decolorization, samples were collected and absorbance of the solution at a λ_{max} equals to 598 nm was measured to monitor the residual TB concentration.

Results and discussion

Thermal study

Figures 2 and 3 show DTA and TGA curves of the thermal decomposition process of LCFO xerogel obtained at a heating rate of 10°C/min in the air from room temperature to 1000°C. The total weight loss of the xerogel was approximately 77% and the decomposition process can be divided into three distinct steps. The first weight loss occurs during the heating step from 150°C

to 255$^°$C (47%), resulting from the dehydration and decomposition of nitrates. In this area, DTA curve shows two exothermic peaks at 141$^°$C and 255$^°$C.From 255$^°$C to about 341$^°$C, a weight loss of about 5% was observed which attributed to the decomposition of chemically bound groups. A weight loss of about 25% is observed from 342$^°$C to about 641$^°$C(25%), which corresponds to the oxidizing combustion of the organic compounds such as citric acid (forming carbonate and oxide with cation) [24,25]. No obvious change was observed above 650$^°$C. Hence, it is plausible to conclude that the optimum calcination temperature is about 750$^°$C.
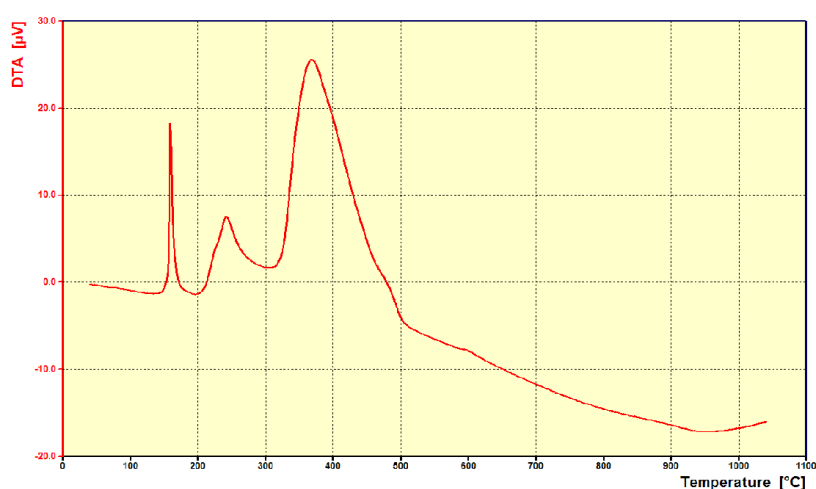
Figure 2. DTA curve of the LCFO precursors obtained by sol–gel Method.
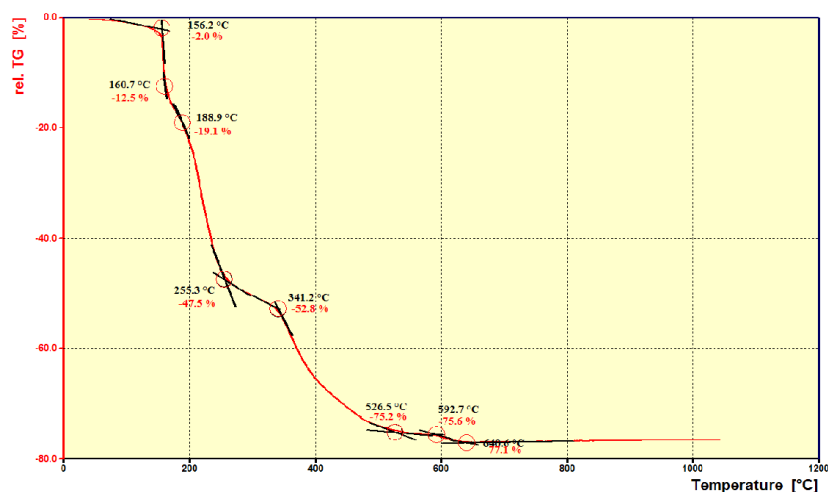

Figure 3. TGA curves of the LCFO xerogel carried out from room temperature to 1000$^°$C in air.

X-ray structural and microscopic analysis

XRD patterns of the synthesized powder which calcined at 750°C for 9 h (heating rate: 3°C/min) is shown in Figure 4. XRD results reveal the existence of a perovskite-type phase for sol-gel method at this temperature. When the precursor was calcined at 750°C for 9 hours, several sharp peaks was observed attributed to the perovskite $LaCo_{0.5}Fe_{0.5}O_3$ by comparison with standard XRD spectra.
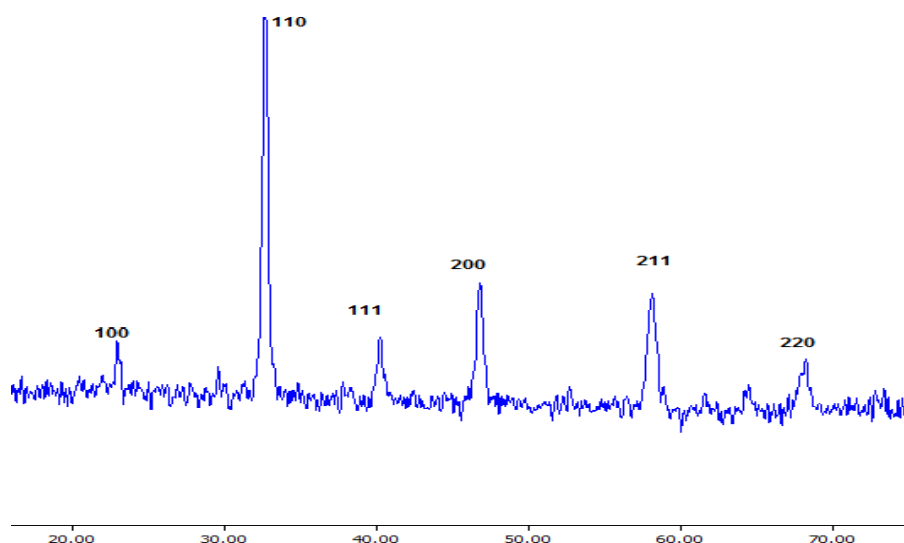

Figure 4. XRD patterns of samples of the LCFO nanopowder calcinatedat 750°C.

The diffraction peaks at 2θ angels appeared in the order of 23.44°, 33.41°, 41.22°, 47.95°, $59.78^{\circ}$and 67.95° can be assigned to scattering from the (10 0), (110), (111), (2 0 0), (21 1)and (2 2 0) planes of the $LaCo_{0.5}Fe_{0.5}O_3$perovskite type crystal lattice, respectively. The crystallite sizes were calculated using XRD peak broadening of the (2θ=33.41) peak by the well-known Scherer's formula (1):

$$D_{hkl} = \frac{0.9\,\lambda}{\beta_{hkl}\,\cos\,\theta_{hkl}} \qquad (1)$$

where D_{hkl} is the particle size perpendicular to the normal line of (hkl) plane, β_{hkl} is the full width at half maximum, θ_{hkl} is the Bragg angle of (hkl) peak, and λ is the wave length of X-ray. The particle sizes of LCFO nanoparticles calcinated at 750°Cwas about 13 nm.

SEM images and EDX analysis

Scanning electron microscopy (SEM) of perovskite oxide (LCFO) prepared by the sol–gel method and calcined at $750^{\circ}C$ is shown in Figure 5. Based on the SEM images, porosity of the surface is evident and it seems that the particles have not grown with uniform size. The particles size of LCFO that were propagated on the surface seems to be in the range of 50–200 nm. The surface looks rough and nearly fully covered with the particles grown on it. Further, it can also be seen from the SEM result that in addition to the larger particles (50–200 nm), the surface contains also rather smaller particles as down to 20 nm or less. However, appearance of bigger particles on the surface looks to be dominant. The aggregation of the smaller particles (in the nm range) may result in bigger LCFO particles on the surface.
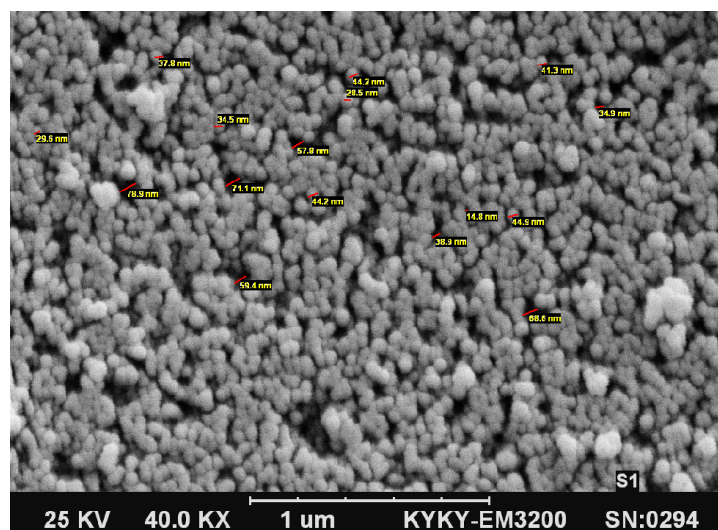

Figure 5. SEM images of LCFO nanopowders.

The EDX analysis was performed to further confirmation of the obtained product composition. Figure 6 shows EDX spectrum which indicates the existence of La, Co, Fe and O elements in this nanoparticle.
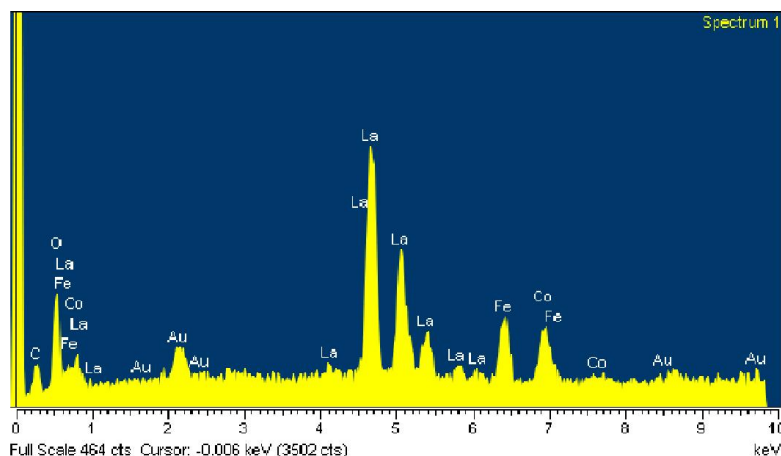
Figure 6. Energy dispersive X-ray (EDX) spectrum of the LCFO nanoparticles.

IR spectra

Fourier transform infrared spectra were obtained for xerogels and nanopowder samples after heating treatment leading to the oxides. Figure 7(a,b) shows the FT-IR spectra of the LCFO powders in the range of 600–4,000 cm^{-1} , fresh xerogels and calcined at 750°C, respectively. The FT-IR spectrum is similar to the most other ABO_3-type perovskite compounds which have common BO_6oxygen octahedral structure [26-28]. Two samples show the typical M–O–C pair vibrations around 1,385 and 1,720 cm^{-1}[29]. The characteristic band at about 1,228 cm^{-1}corresponds to the anti-symmetric NO_3-stretching vibration [30]. A broad band is observed between 3,400 and 3,500 cm^{-1} which corresponds to the O–H stretching vibration [31] due to water species occluded into the gel. The FTIR spectra of calcined sample show the vanishing of bands related to organic and hydroxyl groups. One strong band is observed at~602 cm^{-1}in the FT-IR spectrum. This peak is characteristics of perovskite oxides and can be attributed to M–O stretching [32,33].
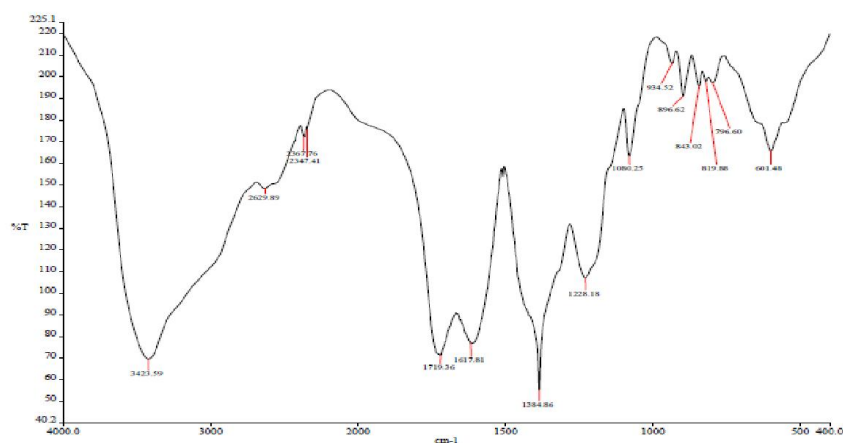
(a)
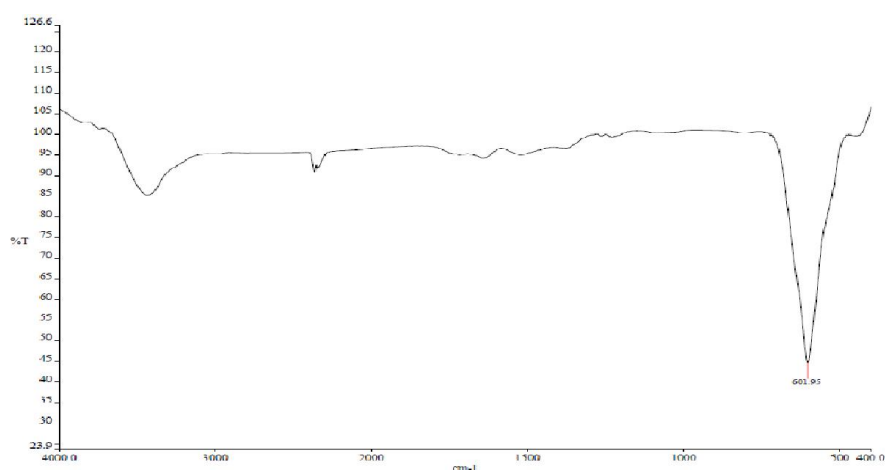
(b)

Figure 7. (a) FT-IR spectra of LCFO xerogel, (b) calcinated powders at 750°C.

Adsorption experiment

The efficiency of the prepared and characterized LCFO nanoparticles as an adsorbent for removal of TB from liquid solutions was investigated using a batch equilibrium technique placing different amount of adsorbent in a glass bottle containing 10 ml of a dye solution at 50 mg/L concentrations. The adsorption studies were carried out for different pH values, contact time, catalyst dosage and dye solution concentrations and results are presented in the following sections.

34

Effect of pH

Solution pH is an important parameter that affects adsorption of dye molecules. The effect of the initial solution pH on the dye removal efficiency of TB by LCFO particles was evaluated at different pH values, ranging from 2 to 12, with a stirring time of 15 min. The initial concentrations of dye and adsorbent dosage were set at 50 mg/L and 0.01 g, respectively. The percentage of dye removal is defined as (2):

$$Removalrate\% = \frac{C_o - C(t)}{C_o} \times 100 \ (2)$$

where C_0 is the initial concentration of TrypanBlueand C_t is concentrationof Trypan Blue at certain reaction time t (min).

As shown in Figure 8, the dye removal was much higher in acidic pH (pH 2), and decreased when the pH was increased from 4 to 12. Since the removal of TB increased to its maximum value at pH 2 (the removal of TB above 96% was achieved) the electrostatic attraction between the dye molecules (negatively charged) and LCFO surface (positively charged) might be the predominant adsorption mechanism. Therefore, to have the optimized condition to remove TB, acidic pH should be applied and pH 2 seems to lead to the best result; so this pH was selected to run further experiments.
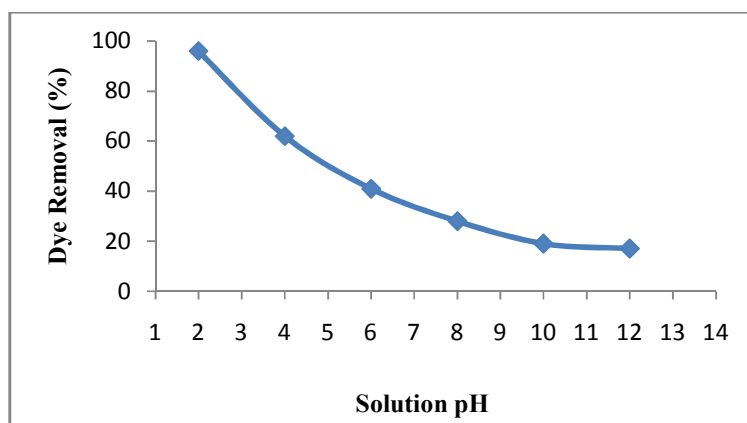

Figure 8. Effect of initial pH of dye solution on removal of Trypan Blue (LCFO dosage 0.01 g, initial dye concentration 50 mg/L, stirring time 15 min).

Effect of contact time and adsorbent dosage

To further assessing of dye removal, the effects of contact time and adsorbent concentration on the removal of TB by LCFO nanoparticles were examined. Initial dye concentrations and pH of the solutions were fixed at 50 mg/L and 2, respectively, for all the batch experiments.

Results are shown in Figure 9. As indicated, increasing of contact time in different dosages of adsorbent led to decrease in the concentration of TB. This behavior was also observed when catalyst dosage increased from 0.005 to 0.02 g. This decreasing in the concentration is due to the adsorption of TB on LCFO nanoparticles and the greater number of adsorption sites for dye molecules made available at greater LCFO dosages. The removal efficiency of TB at the initial dosage of 0.01 g, increased from 77% at the second minute of contact to 96% at time equals to 20 min by keeping constant stirring, however, with increasing LCFO dosage to 0.02 g the percentage of removal obtained in the second minute of stirring was 91%, and the most percent of removal (99%) was attained when the stirring was continued till time equals to 15 min. The catalyst dosage obtained in this study for complete removal of TB on to LCFO powder is less than most of the reported values in the literatures for dye adsorption using other adsorbentdosage used for completeremoval of TB on to LCFO nanopowder is an advantageof this study.
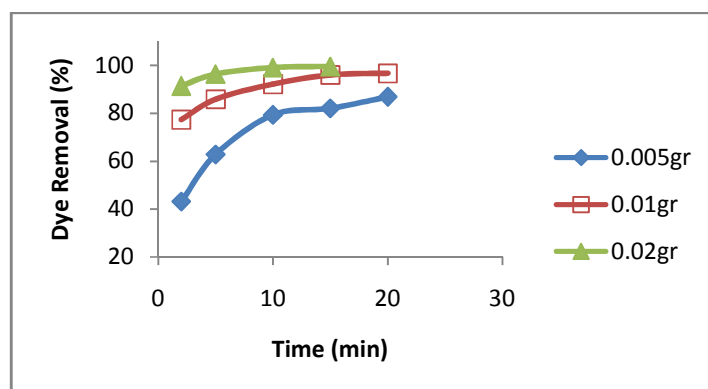

Figure 9. Effect of stirring time on removal of Trypan Blue in different doses (filled diamond) 0.005 g,(filled square) 0.01 g, (filled triangle) 0.02 gof LCFO (initial dye concentration 50 mg/L, initial pH=2).

Effect of dye concentration

The initial dye concentration is another important variable that can affect the adsorption process. The effect of initial TB concentration on dye removal efficiency by LCFO particles was studied by varying the initial dye concentration from 50 to 300 mg/L at pH 2, a catalyst dosage of 0.01g

and contact time of 15 min, as shown in Figure 10. Results show that decolorization of textile dye TB decreases with increasing initial concentration. As it is obvious, the percentage removal of TB decreased from around 96% at a concentration of 50 mg/L to 54% when the concentration was increased to 300 mg/L. This behavior reveals the dependency of adsorption to initial concentration of TB.
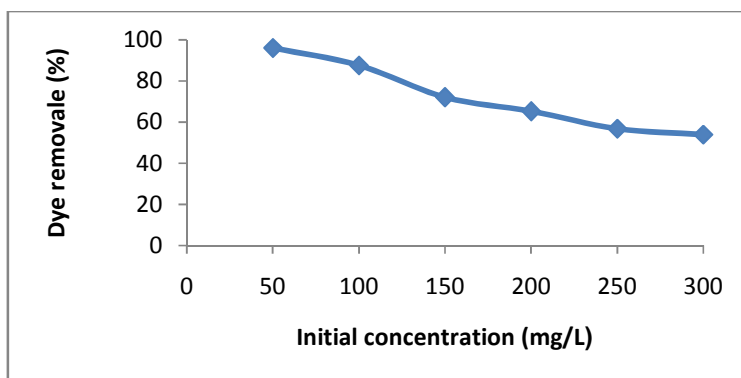

Figure 10. Effect of initial dye concentration on removal of Trypan Blue (LCFO dosage 0.01 g, initial pH 2, stirring time 15 min).

Adsorption kinetic studies

Several models are available to investigate the adsorption kinetics. The first (Eq. 3) and second (Eq. 4)-order reaction rate equations are the most commonly applied models [34,35].To find the suitable chemical removal model for describing the experimental kinetic data, the obtained data were evaluated using first and secondorder reaction rate models.

For the first and second order kinetic model, the experimental data have been fitted with the following equations:

$$\text{First-order equation: } \ln C(t) = \ln C_o - k_1 t \quad (3)$$

$$\text{Second-order equation: } \frac{1}{C(t)} = k_2 t + \frac{1}{C_o} \quad (4)$$

where k_1 and k_2 are the first-order and second-order rate constants, respectively. The plots of experimental results of the two models showed that the removal of dye follows second-order kinetics with rate constant of 0.189 M^{-1} min^{-1}

Adsorption isotherms

The quantity of the dye that could be adsorbed over the nanoperovskites surface is a function of concentration and may be explained by adsorption isotherms. The Langmuir, Freundlich and Temkin isotherm models were applied to the adsorption data. For the equilibrium concentration of adsorbate (C_e) and the amount adsorbed at the equilibrium (q_e), the following forms of the Langmuir (Eq. 5) and Freundlich (Eq. 6) adsorption isotherm equations were used (Eqs. 5, 6):

$$\frac{Ce}{qe} = \frac{1}{K_L q_{max}} + \frac{Ce}{q_{max}} \qquad (5)$$

$$Logqe = LogK_F + \frac{1}{n} LogC_e \qquad (6)$$

where the q_{max} (mg g^{-1}) is the surface concentration atmono-layer coverage which illustrates the maximum value of q_e. The b parameter is a coefficient related to the energy of adsorption and it increases with increasing strength of the adsorption bond [36,37]. K_F and n are constants of the Freundlich equation [38]. The constant KF represents the capacity of the adsorbent for the adsorbate and *n* relates to the adsorption distribution. Moreover, the derivation of the Temkin isotherm assumes that the fall in the heat of adsorption is linear rather than logarithmic, as implied in the Freundlich equation. The Temkin isotherm is as following (Eq. 7):

$$qe = A + BlnCe \qquad (7)$$

where A and B are isotherm constants. The linearized form plots of the Langmuir, Freundlichand Temkin isotherms are shown in Figures 11, 12 and 13. The value of correlation coefficient (R^2) for Freundlich isotherm is greater than that of the Langmuir and Temkin isotherms. This indicates that Freundlich model can describe the adsorption of Trypan Blue on nanoperovskites better than the other models.
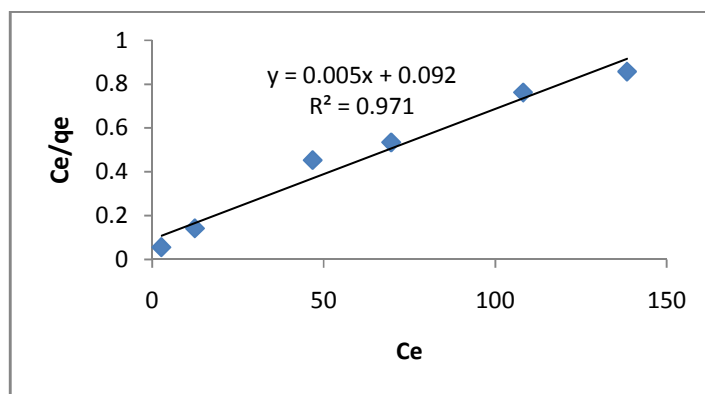
Figure 11. Langmuir isotherm plot of Trypan Blue adsorption onto LCFO nanoparticles: LCFO dosage 0.01 g, initial pH 2, stirring time15 min, initial dye concentration 50, 100, 150, 200, 250, 300 mg/L.

Figure 12. Freundlich isotherm plot of Trypan Blue adsorption onto LCFO nanoparticles: LCFO dosage 0.01 g, initial pH 2, stirring time15 min, initial dye concentration 50, 100, 150, 200, 250, 300 mg/L.
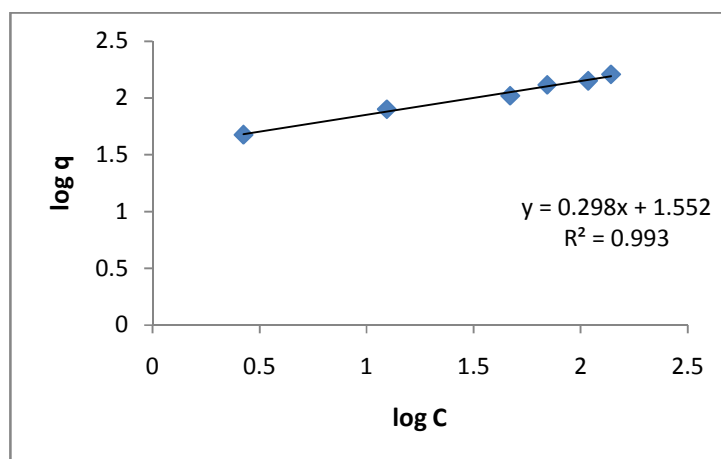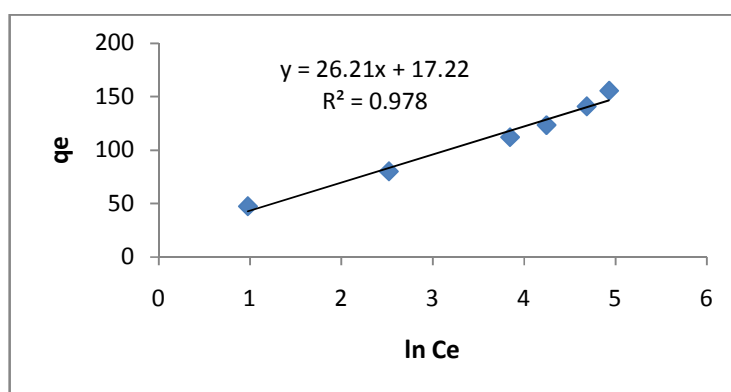

Figure 13. Temkin isotherm plot of Trypan Blue adsorption onto LCFO nanoparticles: LCFO dosage 0.01 g, initial pH 2, stirring time20 min, initial dye concentration 50, 100, 150, 200, 250, 300 mg/L.

Conclusions

The nanoperovskiteLaCo$_{0.5}$Fe$_{0.5}$O$_3$ was prepared by sol–gel method using citric acid. The XRD reveals that the nanoparticles prepared by calcinating the gel precursor at 750°C for 9 h have good crystallinity with fine Hexagonal perovskite structure. In the present study, we demonstrated the nanoperovskites can act as a novel adsorbent material for removal of Trypan Blue. The results showed that the Trypan Blue dye can be successfully removed from aqueous solutions by the nanoperovskites. A first-order model describes the adsorption kinetic data. The equilibrium adsorption can be described using Freundlich model. This adsorbent exhibits either comparable or better performance to the existing adsorbents, already reported by researchers for dye removal from aqueous solutions. Therefore, these nanoperovskite-type oxides are promising candidates for the adsorption of different dyes from wastewaters.

References

[1] S.H. Lin, M. L. Chen, *Water Res*., 31, 868 (1997).

[2] F.P. Van der Zee, R.H.M. Bouwman, D.P. Strik, G. Lettinga, *J.A. Field.*, 75, 691 (2001).

[3] K.T. Chung, S.E.J. Stevens, *Environ Toxicol. Chem*.,12, 2121 (1993).

[4] J.H.Weisburger, *Mutat Res.,*506, 9 (2002).

[5] D.P. Oliveira, P.A. Carneiro, M.K. Sakagami, M.V.B. Zanoni, G.A. Umbuzeiro, *Mutat Res.,*626,135 (2007).

[6] Christie, R., Colour Chemistry, the Royal Society of Chemistry, Cambridge. United Kingdom, 2001.

[7] H. Tavakkoli, F. Sarafion, *J. Appl. Chem. Res*., 11, 95 (2017).

[8]S. Chatterjee, D.S. Lee, M.W. Lee, S.H. Woo, *Bioresour Technol.,*100,3862 (2009).

[9] C.Y. Xia, Y. Jing Jia, D. Yue, J. Ma, X. Yin, *Desalination.,*265,81 (2011).

[10] A.L. Ahmad, S.W. Puasa,*J.Chem. Eng.,*132,257 (2007).

[11]J. Labanda, J. Sabate, J. Llorens, *J. Membr. Sci.,*340, 234 (2009).

[12]M. E. Osugi, K. Rajeshwar, E. R. A. Ferraz, D. P. deOliveira, R. Arojo, M. V. B. Zanoni, *Electrochim.Acta,*54,2086 (2009).

[13]M.B. Kasiri, A.R. Khataee, *Desalination.,*270,151 (2011).

[14]F. Yi, S. Chen, C. Yuan, *J. Hazard. Mater.,*157,79 (2008).

[15]A.R. Tehrani-Bagha, N.M. Mahmoodi, F.M. Menger, *Desalination.,*260,34 (2010).

[16]G. Mezohegyi, F. Goncalves, J.J.M. Orfao, A. Fabregat, A. Fortuny, J. Font, C. Bengoa, F. Stuber, *Appl.Catal. B: Environ.,*94,179 (2010).

[17]A.P. Pantelis, P.X. Nikolaos, M. Dionissios, *Water Res.,*40,1276 (2006).

[18]H. Tavakkoli, T. Moayedipour, *J. Nanostruct. Chem.*, 4, 1 (2014).

[19]H.D. Mansill, C. Bravo, R. Ferreyra, M.I. Litter, W.F. Jardim, C. Lizama, J. Freer, J. Fernandez, *J. Photochem. Photobiol. A. Chem.*, 181,188 (2006).

[20] D.B. Meadowcroft, *Nature.,*226,847 (1970).

[21]Y. Zhu, R. Tan, T. Yi, S. Ji, X. Ye, L. Cao, *J. Mater. Sci.,*35, 5415 (2000).

[22]M. Yazdanbakhsh, H. Tavakkoli, S. M. Hosseini, *S. Afr. J. Chem.*, 64, 71 (2011).

[23]E. M. G. De La Cruz, H. Falcon, M. A. Pena, J. L. G. Fierro, *Appl. Catal. B:Environ.,*33,45 (2001).

[24]C. F. Kao, C. L. Jeng, *Ceram. Int.,*25,375 (1999).

[25]C.F. Kao, C.L. Jeng,*Ceram. Int.,*26,237 (2000).

[26]E.R. Leite, C.M.G. Sousa, E. Longo, J.A. Varela, *Ceram. Int.,* 21,143 (1995).

[27]W. Nimmo, N.J. Ali, R.M. Brydson, C. Calvert, E. Hampartsoumian, D. Hind, S.J. Milne, *J.Am. Ceram. Soc.,*86,1474 (2003).

[28]A. Sakar-Deliormanl, E. Celik, M. Polat, *Ceram. Int.,*35,503 (2009).

[29]J. Kim, I. Honma, *Electrochim.Acta.,*49,3179 (2004).

[30]S. Liu, X. Qian, J. Xiao, *J. Sol-Gel. Sci. Technol.,*44,187 (2007).

[31]P.N. Kuznetsov, L.I. Kuznetzova, A.M. Zhyzhaev, G.L. Pashkov, V.V. Boldyrev, *Appl.Catal.A.,*227,299 (2002).

[32]R.N. Singh, B. Lal, *Int. J. Hydrogen Energy.,*27,45 (2000).

[33]Y. Hao, J. Li, X. Yang, X. Wang, L. Lu, *Mater. Sci.Eng. A.,*367,243 (2004).

[34]C.L. Hsueh, Y.W. Lu, C.C. Hung, Y.H. Huang, C.Y. Chen, *DyesPigm.,*75,130 (2007).

[35]D.M. Indra, C.S. Vimal, K.A. Nitin, *Dyes Pigm.,*69,210 (2006).

[36]D. E. Kritikos, N.P. Xekoukoulotakis, E. Psillakis, D. Mantzavinos, *Water Res.,*41,2236 (2007).

[37]I. Langmuir, *J. Am. Chem. Soc.,*40,1361 (1918).

[38]H.M.F Freundlich, Z. *Phys.Chem. A.,*57, 385 (1906).